



Theoretical Study of the Chemical Reactivity of a Series of 2, 3-Dihydro-1H-Perimidine

Nanou Tieba Tuo^a, Georges Stephane Dembele^{a,b*}, Soro Doh^a,
Fandia Konate^a, Bibata Konate^{a,b}, Charles Guillaume Kodjo^{a,c}
and Nahosse Ziao^{a,b}

^a *Laboratoire de Thermodynamique et de Physico-Chimie du Milieu, UFR SFA, Université Nangui Abrogoua 02 BP 801 Abidjan 02, Côte-d'Ivoire.*

^b *Groupe Ivoirien de Recherches en Modélisation des Maladies (GIR2M), Université Nangui Abrogoua, Abidjan, Côte-d'Ivoire.*

^c *Laboratoire de Chimie Bio Organique et de Substances Naturelles, Université Nangui Abrogoua, UFR-SFA, 02 B.P. 801 Abidjan 02, Côte-d'Ivoire.*

Authors' contributions

This work was carried out in collaboration among all authors. All authors read and approved the final manuscript.

Article Information

DOI: 10.9734/IRJPAC/2022/v23i130451

Open Peer Review History:

This journal follows the Advanced Open Peer Review policy. Identity of the Reviewers, Editor(s) and additional Reviewers, peer review comments, different versions of the manuscript, comments of the editors, etc are available here: <https://www.sdiarticle5.com/review-history/81510>

Review Article

Received 22 October 2021
Accepted 19 December 2021
Published 28 January 2022

ABSTRACT

This reactivity study was performed on seven molecules of a 2,3-dihydro-1H-perimidine series using density functional theory at the B3LYP / 6-311 G (d, p) level. Calculation of the dipole moment showed that compound 4 is more soluble in aqueous medium. The study of frontier molecular orbitals, in particular the energy gap (ΔE), electronegativity (χ), chemical hardness (η) and the electrophilic index (ω) has provided a better overview molecular properties. Thus, the compound 5 with the highest energy gap between the boundary orbitals is the most stable and the least reactive. Analysis of local descriptors and the electrostatic potential map identified nitrogen atoms N₂₆ and N₂₈ as the preferred sites of electrophilic attack and the carbon atom C26 as the preferred site of nucleophilic attack.

Keywords: Reactivity; 2,3-dihydro-1H-perimidine; Fukui function; natural charge; DFT.

*Corresponding author: E-mail: 1997sageme@gmail.com;

1. INTRODUCTION

Heterocycles are chemical compounds consisting of rings in which one or more carbon atoms have replaced by a heteroatom such as nitrogen, oxygen, phosphorus, sulfur, etc. These chemical compounds are of great scientific interest because of their potential for application in many fields. The most well-known are heterocycles containing nitrogen and oxygen atoms [1]. Among others, 2,3-dihydro-1*H*-Perimidines are defined as the product resulting from the condensation of 1,8-diaminonaphthalene (1,8 - DAN) with carbonyl derivatives (Aldehyde). The 1*H*-perimidines are a class of heterocyclic compounds which have great structural variety. This allows their use in various scientific fields. They are characterized by either a bond deficit or an excess π bond due to the electron density movements of the nitrogen atoms present in the fused ring system [2]. These compounds have a of ongoing interest because of their polyvalent [3], optoelectronic, chemotherapeutic, thermochromic, and photochromic properties. In this work, a series of seven (7) molecules of 2,3-dihydro-1*H*-perimidine were used (Table 1). The aim of this work is to theoretically determine, on the one hand, the reactivity of these 2,3-dihydro-1*H*-perimidine derivatives and on the other hand to

identify the likely sites of nucleophilic / electrophilic attacks by different methods of quantum chemistry.

2. MATERIALS AND METHODS

2.1 Natural Population Analysis

The determination of the natural atomic charge is essential for the study of molecular systems in quantum chemistry. For the quantitative description of a molecular charge distribution, the compound is divided into well-defined atomic fragments. The objective is to share the charge density at each point between the different atoms in proportion to their free atom densities at the corresponding distances from the nuclei [4]. In our manuscript, the atomic charge values were calculated from the natural population analysis (NPA). The optimization of the geometry of the molecules was done by the DFT calculation method with the B3LYP function [5] in the basis 6-311G (d, p) using the Gaussian 09 [6]. This Hybrid functional gives better energies and is in line with high-level ab initio methods [7]. The geometries are conserved for cationic and anionic systems at computational level B3LYP/6-311G (d, p) to which a calculation of energy has been made.

Table 1. Molecular structures of 2,3-dihydro-1*H*-perimidines studied

Compounds	Structures	Compounds	Structures
1		2	
3		4	
5		6	
7			

2.2 Frontier Molecular Orbitals Theory

The frontier molecular orbital is fundamental in the visualization of chemical reactivity [8]. The most occupied molecular orbital (HOMO) is the highest orbital containing electrons and tends to give up these electrons. On the other hand, the lowest unoccupied molecular orbital (LUMO) is the lowest orbital containing vacant slots to accept electrons. While the HOMO energy is directly related to the ionization potential, the LUMO energy is directly related to the electron affinity. The difference in energy between HOMO and LUMO is called the energy gap and represents an indicator of stability for molecules. The HOMO-LUMO energy gap allows to characterize the chemical reactivity and the chemical stability of the molecule. [8]. A molecule with a high energy gap (ΔE) is less polarizable and is generally associated with low chemical reactivity and high kinetic stability [9]

2.3 Reactivity Descriptors

2.3.1 Global descriptors

In order to predict the reactivity and chemical stability of the compounds the quantum descriptors related to the conceptual DFT were determined: (ionization potential (I), electron affinity (A), electronegativity (χ), global softness (s), global hardness (η) and global electrophilicity (ω)) [10]. The different descriptors quoted have been calculated from the optimized molecules. The descriptors related to the molecular boundary orbitals have been calculated by the Koopmans approximation method [11]. The LUMO energy characterizes the capacity of the molecule to a nucleophilic attack, and as for the HOMO energy it characterizes the capacity of a molecule to an electrophilic attack. The electronegativity (χ) reflects the capacity of a molecule to attract electrons. The global softness (s) expresses the capacity of a system to the modification of its electron number. The global electrophilicity index characterizes the electrophilic power of the molecule. These different descriptors are determined from the equations (1):

$$\begin{aligned} I &= -E_{HOMO} \\ A &= -E_{LUMO} \\ \chi &= -\mu = -1/2 (E_{LUMO} + E_{HOMO}) \\ \eta &= (E_{LUMO} - E_{HOMO})/2 \\ \omega &= \frac{\chi^2}{2\eta} \\ \sigma &= 1/\eta \end{aligned} \quad (1)$$

The chemical potential (μ) characterizes the tendency of the electron to escape from equilibrium. With respect to overall hardness, it measures the resistance to deformation of atoms, ions, or molecules under the influence of the chemical reaction. Parr et al. initiated the concept of electrophilicity as an index of overall reactivity similar to chemical hardness and chemical potential.

2.3.2 Local and dual descriptors

The Fukui indices of a molecule allow to determine the local reactivity of this molecule. The atom with the highest Fukui number is more reactive than the other atoms in the molecule [12]. These indices are the qualitative interpretation of the reactivity of the atoms in the molecule. The Fukui function predicts the local reactivity for most chemical systems with some reliability. We calculated Fukui indices to determine the selectivity of electrophilic and nucleophilic atoms in perimidine compounds. Ayers and Parr [13] explained that molecules tend to react where Fukui's function is greatest when attacked by soft reagents and in places where Fukui's function is smaller when attacked by hard reagents. Using the natural atomic charge of the ground state optimized compounds, the Fukui function (f_k^+ , f_k^-), the local softness (s_k^+ , s_k^-) and the local electrophilia indices (ω_k^+ , ω_k^-) [14] have been determined. The functions of Fukui are calculated using equation (2):

$$\begin{aligned} f_k^+ &= q_k(N+1) - q_k(N) \\ f_k^- &= q_k(N) - q_k(N-1) \end{aligned} \quad (2)$$

f_k^+ : for nucleophilic attack

f_k^- : for electrophilic attack

$q_k(N)$: Electron population of the atom k in the neutral molecule.

$q_k(N+1)$: Electron population of the atom k in the anionic molecule.

$q_k(N-1)$: Electron population of the atom k in the cationic molecule.

Local softness and electrophilicity indices are calculated using (3)

$$\begin{aligned} s_k^+ &= s f_k^+ \\ s_k^- &= s f_k^- \\ \omega_k^+ &= \omega f_k^+ \\ \omega_k^- &= \omega f_k^- \end{aligned} \quad (3)$$

The values of the dual descriptors [15] are obtained from the equations (4)

$$\Delta f = f_k^+ - f_k^- \quad (4)$$

3. RESULTS AND DISCUSSION

3.1 Dipoles Moment of Compounds μ (D)

The dipole moment is an essential parameter for the prediction of the solubility of compounds in aqueous medium. The values of the dipole moment are reported in Table 2.

The dipole moment values of the compounds range from 0.793 Debye to 4.828 Debye. The decreasing order of the dipole moment of the compounds is as follows:

μ (Compound 5) > μ (Compound 7) > μ (Compound 3) > μ (Compound 6) > μ (Compound 4) > μ (Compound 2) > μ (Compound 1).

The order shows us that compound 5 has the greatest dipole moment value. Compound 5 is therefore more soluble in aqueous medium.

3.2 Analysis of Frontier Molecular Orbital

The values of the HOMO and LUMO frontier molecular orbitals of 2,3-dihydro-1H-perimidine obtained by the B3LYP/6-311G method (d, p) are presented in the table below.

The values in the table show compound 2 has the smallest value of the energy gap ($\Delta E_{\text{gap}} = 2.926$ eV), therefore it is the most reactive one consequently it presents a low chemical stability compared to all the studied molecules. On the other hand, compound 4 has the largest value of the energy gap ($\Delta E_{\text{gap}} = 5.969$ eV), therefore it is the least reactive and therefore the most stable compound.

3.3 Reactivity Descriptors

3.3.1 Global reactivity descriptors

The overall reactivity indices of the studied 2,3-dihydro-1H-perimidine were calculated from equations (1) and placed in Table 4.

Compound 2 shows a value of the overall hardness ($\eta = 1.463$ eV), this value is the lowest of all the molecules. Thus, we can say compound 2 is the most reactive out of all the compounds studied. Moreover, we notice that compound 2 has a significantly higher electronegativity value ($\chi = 3.421$ eV) than the other compounds; it then appears as the best electron acceptor. Moreover, the electrophilic index value of compound 2 ($\omega = 4.000$ eV) indicates that it is the most electrophilic.

Table 2. Dipoles moment of compounds

compounds	1	2	3	4	5	6	7
μ (D)	0.793	4.077	4.618	4.154	4.828	4.180	4.758

Table 3. Energy parameters of the compounds studied

compounds	E_{HOMO} (eV)	E_{LUMO} (eV)	ΔE_{gap} (eV)	EI (eV)	A (eV)
1	-4.905	-1.597	3.308	4.905	1.597
2	-4.884	-1.958	2.926	4.884	1.958
3	-4.838	-1.276	3.562	4.838	1.276
4	-4.790	1.179	5.969	4.790	-1.179
5	-4.759	-0.547	4.211	4.759	0.547
6	-4.812	-1.739	3.073	4.812	1.739
7	-4.731	-0.670	4.060	4.731	0.670

Table 4. Global descriptors of chemical reactivity of 2,3-dihydro-1H-perimidine 1-

compounds	μ (eV)	η (eV)	ω (eV)	χ (eV)	s (eV ⁻¹)
1	-3.251	1.654	3.195	3.251	0.605
2	-3.421	1.463	4.000	3.421	0.683
3	-3.057	1.781	2.623	3.057	0.561
4	-1.806	2.985	0.546	1.806	0.335
5	-2.653	2.106	1.671	2.653	0.475
6	-3.276	1.537	3.491	3.276	0.651
7	-2.701	2.030	1.796	2.701	0.493

3.3.2 Local reactivity descriptors

3.3.2.1 Molecular electrostatic potentials and Fukui functions

Regions of electrostatic surface potential are represented by colors ranging from red to blue. The potential increases in the following order: red < orange < yellow < green < blue, where red

indicates the most negative potentials and blue the most positive potentials [16] passing successively through orange, yellow and green. The surfaces of the electrostatic potentials of the studied molecules were represented after optimization at the level DFT/B3LYP / 6-311 G (d, p). They are presented in Fig. 1 obtained from Gaussian 09 [6].

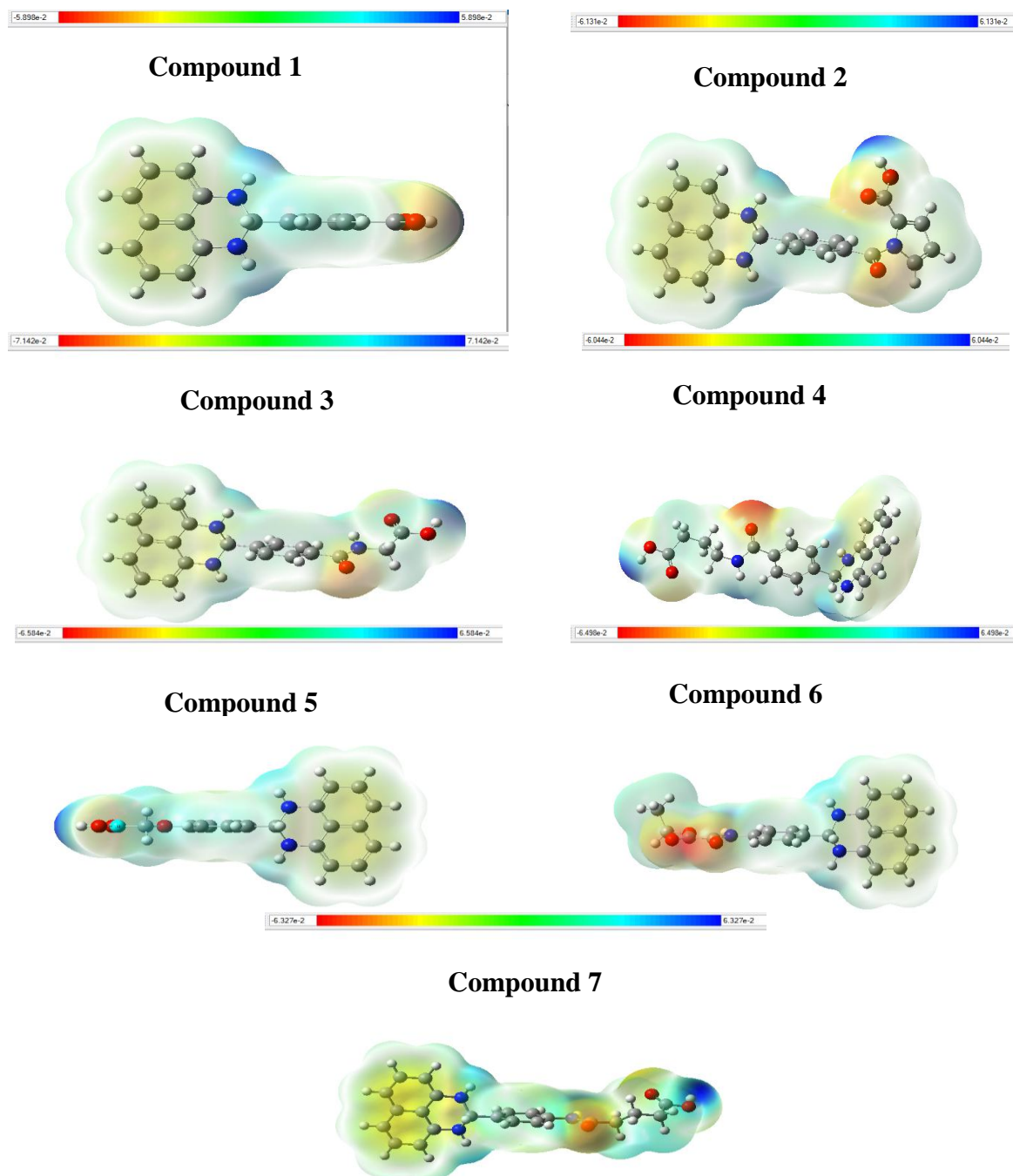


Fig. 1. Surface of molecular Electrostatic potentials of 2,3-dihydro-1H-perimidine

We also determined the local reactivity indices for each molecule according to equations (2), (3) and (4). All the atoms of the compounds are concerned in this study except the hydrogen atoms. These different local indices and reactivity descriptors are grouped in Tables 5 to 11.

The values of the local descriptors of compound 1 calculated at B3LYP/6-311G (d, p) show that the N26 and N28 nitrogen atoms are the preferred sites of electrophilic attack. According to this same level of calculation, nucleophilic attack will preferentially occur on the C32 atom with a value in Table 5.

The results in Table 6 predict that the N₂₈ and N₃₀ azote atoms are most favored to attack electrophilic species. As regards the nucleophilic attack, it occurs preferentially on carbon C₂₆.

In the Table 7, the azote atoms N₂₈ and N₃₀ are most favored for electrophilic attack. As regards the nucleophilic attack, are occurs preferentially on C₂₆ and C₃₉ carbon.

Table 8 predicts that the N₂₈ and N₃₀ azote atoms are most favored against electrophilic attacks. As regards the nucleophilic attack, are occurs preferentially on C₂₆ and C₄₅ carbons.

The results in Table 9 predict that the N₂₆ and N₂₈ azote atoms are most favored for

electrophilic attacks. As regards the nucleophilic attack, it occurs preferentially on carbon C₃₆.

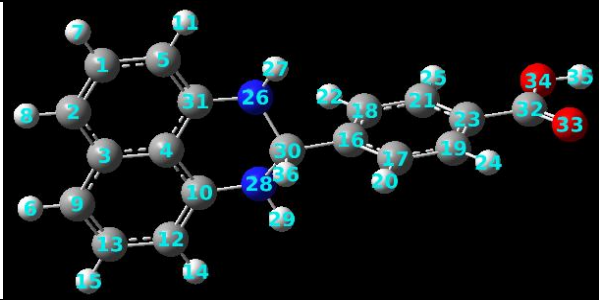
The values of the local descriptors calculated show that the azote atoms N₂₆ and N₂₈ are the preferred sites of electrophilic attack. According to this same level of calculation, a nucleophilic attack will preferably take place on the C₃₂ atom having a value in the Table 10.

In the Table 11, the azote atoms N₂₆ and N₂₈ are most favored for electrophilic attack. As regards the nucleophilic attack, it occurs preferentially on C₄₅ carbon.

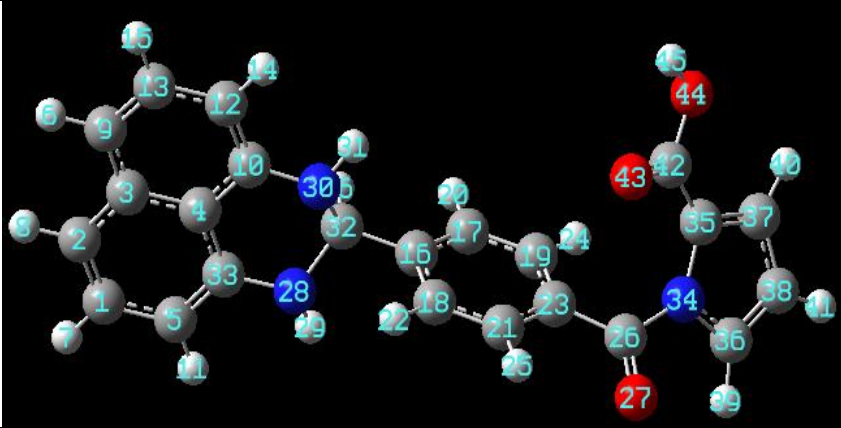
3.3.2.2 Dual reactivity descriptors

The numerical values of the dual reactivity descriptor were also determined for each molecule according to (2). All the constituent atoms of the different compounds are concerned in this study with the exception of the hydrogen atoms. These different local indices and descriptors of reactivity are grouped together in graphs 1 to 6. The numerical values of the double descriptor of the compounds were calculated at the level B3LYP / 6-311 G (d, p), show that the nitrogen atoms N₂₆ and N₂₈ for some compounds and N₂₈ and N₃₀ for others are generally the preferred sites of electrophilic attack.

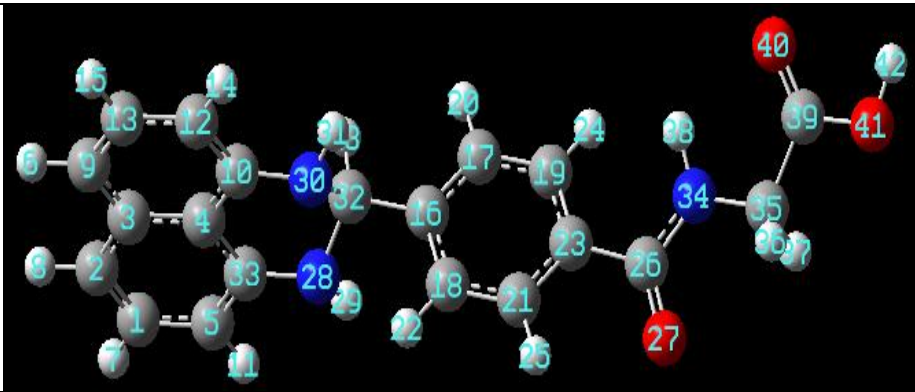
Table 5. Compound 1 reactivity descriptors calculated using natural population analysis (NPA)



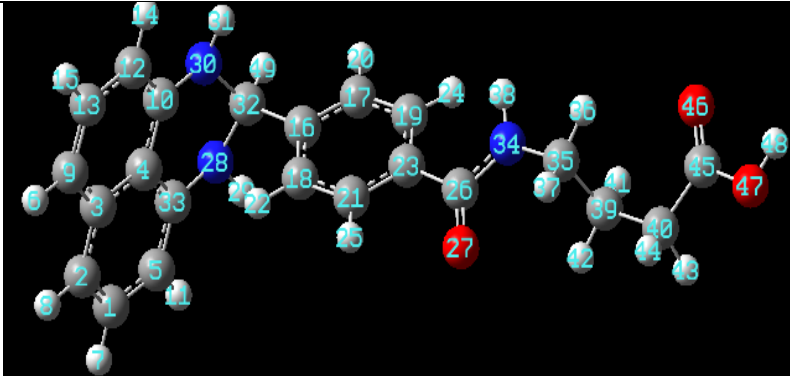
Sites	Local descriptors							
	f+	f-	ω+	ω-	s+	s-	η+	η-
C32	0.523	-0.419	0.966	-0.773	0.252	-0.201	0.602	-0.482
C10	0.128	-0.041	0.237	-0.076	0.062	-0.020	0.148	-0.048
C31	0.128	-0.041	0.237	-0.076	0.062	-0.020	0.148	-0.048
C30	0.079	-0.073	0.145	-0.135	0.038	-0.035	0.090	-0.084
C16	0.133	0.006	0.245	0.010	0.064	0.003	0.153	0.006
C3	-0.027	-0.027	-0.049	-0.049	-0.013	-0.013	-0.031	-0.031
C5	-0.131	0.278	-0.241	0.512	-0.063	0.134	-0.150	0.320
O33	-0.200	0.310	-0.368	0.572	-0.096	0.149	-0.230	0.357
O34	-0.324	0.355	-0.597	0.655	-0.156	0.171	-0.372	0.408
N28	-0.312	0.419	-0.576	0.774	-0.150	0.202	-0.359	0.482
N26	-0.312	0.419	-0.576	0.774	-0.150	0.202	-0.359	0.482

Table 6. Compound 2 reactivity descriptors calculated using natural population analysis (NPA)


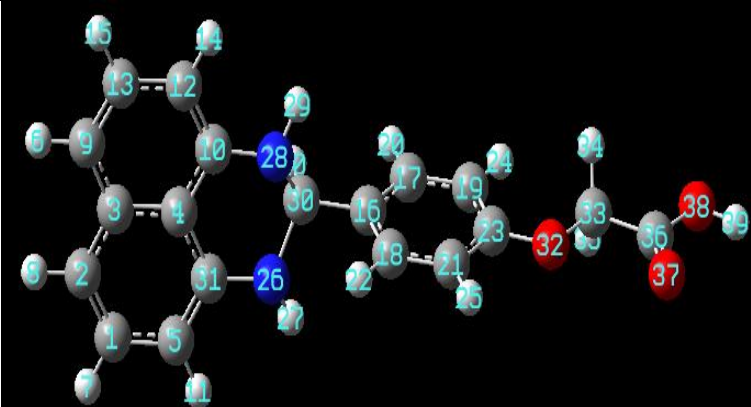
Sites	Locals descriptors							
	f+	f-	ω^+	ω^-	s+	s-	η^+	η^-
C26	0.538	-0.367	0.993	-0.677	0.259	-0.176	0.619	-0.422
C42	0.425	-0.025	-0.450	0.476	-0.900	0.926	0.489	-0.029
C10	0.103	-0.043	0.190	-0.079	0.049	-0.021	0.118	-0.049
C33	0.103	-0.043	0.190	-0.079	0.049	-0.021	0.118	-0.049
C32	0.071	-0.073	0.132	-0.134	0.034	-0.035	0.082	-0.084
N34	-0.224	0.198	-0.413	0.366	-0.108	0.095	-0.258	0.228
O33	-0.277	0.296	-0.511	0.547	-0.133	0.142	-0.318	0.341
O34	-0.340	0.356	-0.627	0.657	-0.163	0.171	-0.391	0.410
N28	-0.319	0.418	-0.589	0.772	-0.153	0.201	-0.367	0.481
N30	-0.320	0.420	-0.590	0.776	-0.154	0.202	-0.368	0.484

Table 7. Compound 3 reactivity descriptors calculated using Natural Population Analysis (NPA)


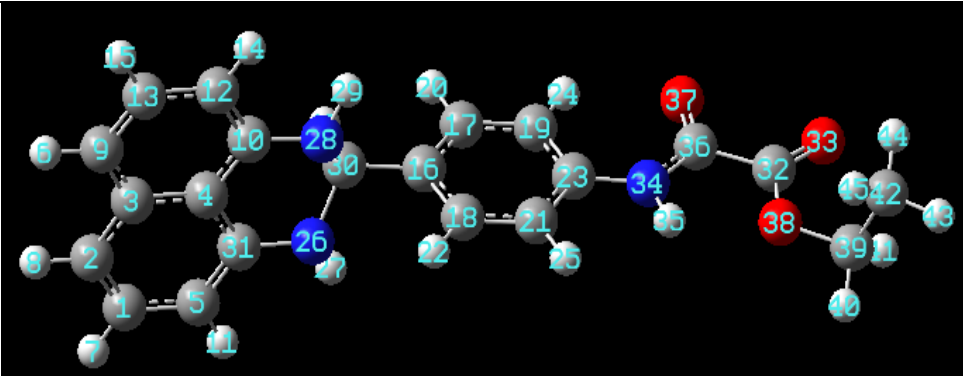
Sites	Locals descriptors							
	f+	f-	ω^+	ω^-	s+	s-	η^+	η^-
C26	0.417	-0.345	0.770	-0.636	0.201	-0.166	0.480	-0.397
C39	0.428	-0.004	-0.432	0.435	-0.863	0.867	0.492	-0.004
C10	0.138	-0.043	0.255	-0.080	0.067	-0.021	0.159	-0.050
C33	0.138	-0.043	0.256	-0.080	0.067	-0.021	0.159	-0.050
C32	0.083	-0.073	0.153	-0.136	0.040	-0.035	0.095	-0.085
O40	-0.299	0.303	-0.552	0.559	-0.144	0.146	-0.344	0.348
N34	-0.297	0.328	-0.549	0.605	-0.143	0.158	-0.342	0.377
O41	-0.341	0.351	-0.630	0.647	-0.164	0.169	-0.393	0.404
N30	-0.310	0.419	-0.572	0.774	-0.149	0.202	-0.357	0.483
N28	-0.310	0.420	-0.573	0.775	-0.1493	0.202	-0.357	0.483

Table 8. Compound 4 reactivity descriptors calculated using Natural Population Analysis (NPA)


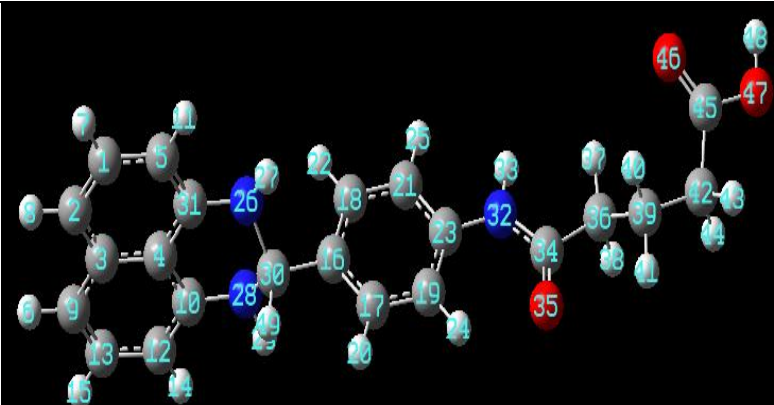
Sites	Locals descriptors							
	f+	f-	ω^+	ω^-	s+	s-	η^+	η^-
C26	0.401	-0.349	0.740	-0.644	0.193	-0.168	0.462	-0.402
C45	0.437	-0.010	-0.447	0.46	-0.894	0.904	0.503	-0.012
C10	0.140	-0.052	0.258	-0.096	0.067	-0.025	0.161	-0.060
C33	0.139	-0.050	0.257	-0.093	0.067	-0.024	0.160	-0.058
C32	0.076	-0.077	0.141	-0.143	0.037	-0.037	0.088	-0.089
O46	-0.301	0.303	-0.556	0.559	-0.145	0.146	-0.347	0.349
N34	-0.297	0.333	-0.549	0.614	-0.143	0.160	-0.342	0.383
O47	-0.345	0.354	-0.636	0.654	-0.166	0.170	-0.397	0.408
N30	-0.307	0.414	-0.567	0.764	-0.148	0.199	-0.353	0.476
N28	-0.308	0.416	-0.568	0.768	-0.148	0.200	-0.354	0.479

Table 9. Compound 5 reactivity descriptors calculated using Natural Population Analysis (NPA)


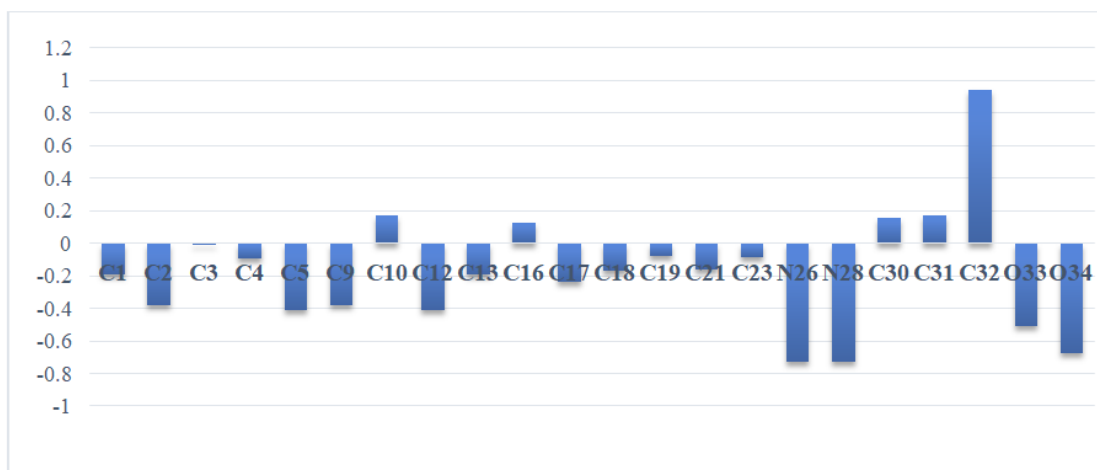
Sites	Locals descriptors							
	f+	f-	ω^+	ω^-	s+	s-	η^+	η^-
C36	0.496	-0.078	-0.574	0.652	-1.148	1.226	0.571	-0.090
C23	0.165	-0.155	0.3045	-0.286	0.079	-0.075	0.190	-0.179
C31	0.188	-0.046	0.347	-0.085	0.090	-0.022	0.216	-0.053
C10	0.188	-0.046	0.347	-0.085	0.090	-0.022	0.216	-0.053
C30	0.089	-0.074	0.164	-0.137	0.043	-0.036	0.102	-0.086
O32	-0.244	0.258	-0.450	0.477	-0.117	0.124	-0.281	0.298
O37	-0.238	0.286	-0.440	0.528	-0.115	0.138	-0.274	0.329
O38	-0.342	0.359	-0.632	0.663	-0.165	0.173	-0.394	0.413
N28	-0.310	0.419	-0.573	0.774	-0.149	0.202	-0.357	0.483
N26	-0.310	0.419	-0.573	0.774	-0.149	0.202	-0.357	0.483

Table 10. Compound 6 reactivity descriptors calculated using Natural Population Analysis (NPA)


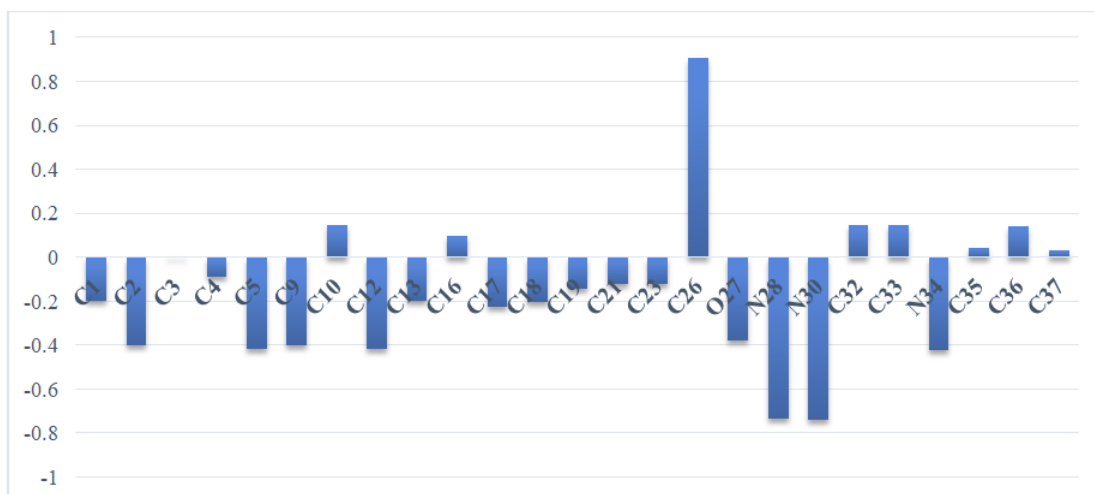
Sites	Locals descriptors							
	f+	f-	ω^+	ω^-	s+	s-	η^+	η^-
C32	0.494	-0.120	-0.615	0.735	-1.230	1.350	0.569	-0.139
C36	0.433	-0.137	-0.570	0.706	-1.140	1.276	0.499	-0.157
C23	0.120	-0.070	0.222	-0.129	0.058	-0.033	0.138	-0.080
C31	0.126	-0.045	0.233	-0.082	0.061	-0.021	0.145	-0.051
C10	0.126	-0.045	0.233	-0.082	0.061	-0.021	0.145	-0.051
O33	-0.163	0.279	-0.300	0.516	-0.078	0.134	-0.187	0.322
O38	-0.262	0.288	-0.484	0.532	-0.126	0.139	-0.302	0.331
N34	-0.317	0.305	-0.585	0.564	-0.152	0.147	-0.365	0.352
N28	-0.315	0.420	-0.582	0.776	-0.152	0.202	-0.363	0.484
N26	-0.315	0.420	-0.582	0.775	-0.152	0.202	-0.363	0.483

Table 11. Compound 7 reactivity descriptors calculated using Natural Population Analysis (NPA)


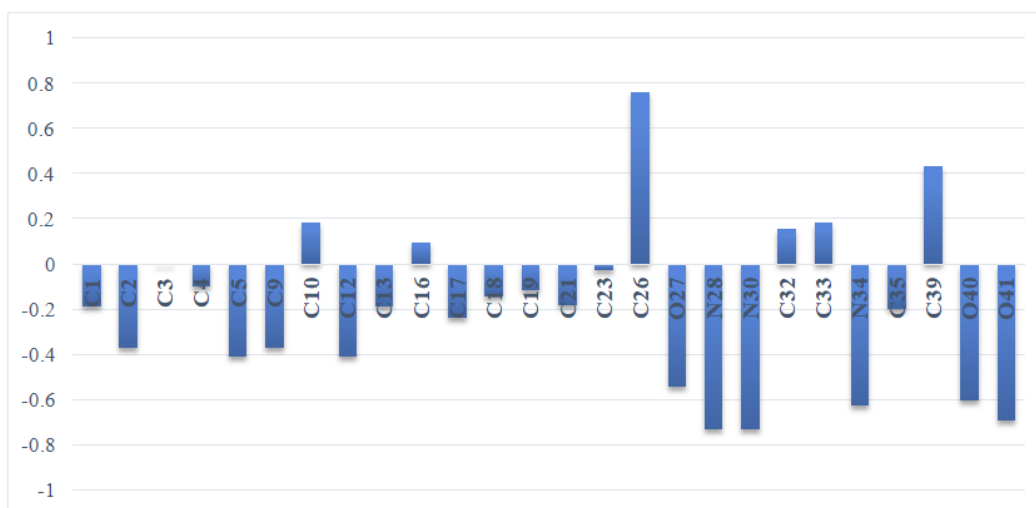
Sites	Locals descriptors							
	f+	f-	ω^+	ω^-	s+	s-	η^+	η^-
C45	0.520	-0.094	-0.614	0.708	-1.229	1.323	0.599	-0.108
C34	0.429	-0.071	-0.500	0.571	-1.000	1.071	0.493	-0.082
C23	0.146	-0.073	0.270	-0.134	0.070	-0.035	0.169	-0.084
C10	0.160	-0.047	0.295	-0.086	0.077	-0.022	0.184	-0.054
C31	0.160	-0.047	0.295	-0.086	0.077	-0.022	0.184	-0.054
O46	-0.299	0.301	-0.553	0.556	-0.144	0.145	-0.345	0.347
N32	-0.324	0.311	-0.599	0.574	-0.156	0.149	-0.373	0.358
O47	-0.325	0.354	-0.600	0.654	-0.156	0.170	-0.374	0.408
N28	-0.308	0.420	-0.568	0.775	-0.148	0.202	-0.354	0.483
N26	-0.308	0.420	-0.568	0.776	-0.148	0.202	-0.354	0.484



Graph 1. Dual descriptor (Δf) of compound 1



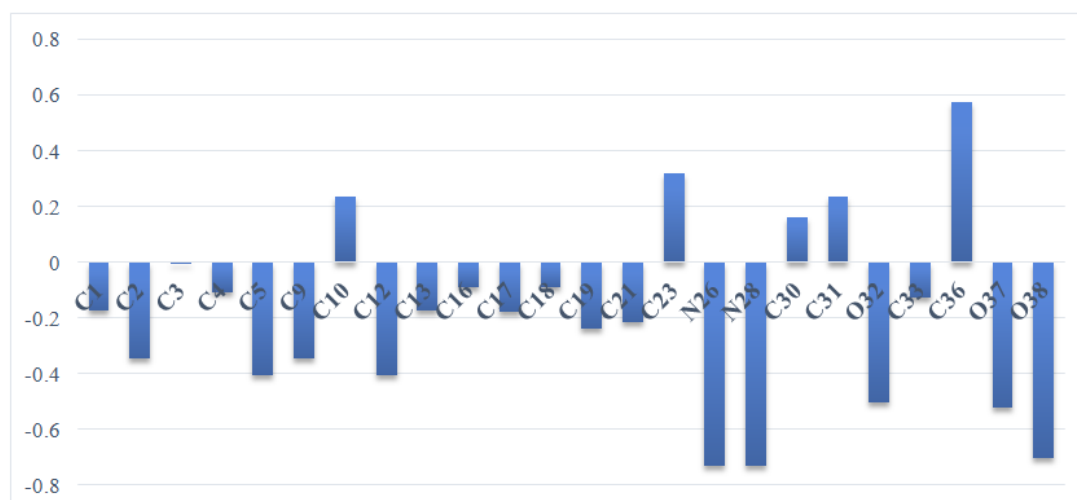
Graph 2. Dual descriptor (Δf) of compound 2



Graph 3. Dual descriptor (Δf) of compound 3



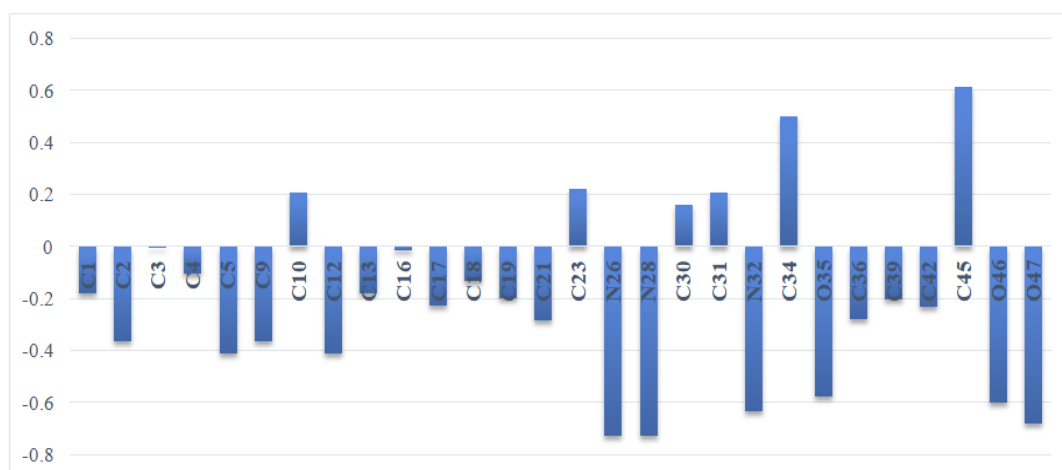
Graph 4. Dual descriptor (Δf) of compound 4



Graph 5. Dual descriptor (Δf) of compound 5



Graph 6. Dual descriptor (Δf) of compound 6



Graph 7. Dual descriptor (Δf) of compound 7

4. CONCLUSION

In this work, the methods of Quantum Chemistry and Molecular Modeling were used on seven (7) molecules of the 2,3-dihydro-1H-perimidine family with a view to study their reactivity. The dipole moment, global and local descriptors were used to study the reactivity of different nucleophilic, electrophilic and radical sites. The dipole moment showed that compound 5 is more soluble in aqueous medium. As for the global descriptors; they revealed that compound 4 is more stable and less reactive. Analysis of local descriptors confirmed the likely sites of electrophilic and nucleophilic attack. In order to accurately determine the sites of attack, the Fukui indices and dual descriptors were calculated from the Natural Population Analysis (NPA). The latter showed that for the series of molecules studied, nitrogen atoms N₂₆ and N₂₈ are the privileged sites of electrophilic attack and the carbon atom C₂₆ is the preferential site of nucleophilic attack.

COMPETING INTERESTS

Authors have declared that no competing interests exist.

REFERENCES

1. Abdelmadjid H. Synthèse des hétérocycles azotés à cinq chaînons dérivés de l'acide sorbique et détermination de leurs activités biologiques us to;2013.
2. Harry NA, Radhika S, Neetha M, Anilkumar G. A novel catalyst-free mechanochemical protocol for the synthesis of 2,3-dihydro-1H-perimidines. *J. Heterocycl. Chem.* 2020;13:2–8.
3. Giani AM. Fluorescence studies on 2-(het)aryl perimidine derivatives. *J. Lumin.* 2016;179:384–392.
4. Hirshfeld FL. Bonded-atom fragments for describing molecular charge densities. *Theor. Chim. Acta.* 1977;44(n° 12):129–138.
5. Becke A. Density-functional thermochemistry III. The role of exact exchange. *Journal of Chemistry Physical.* 1993;98(n° 17):5648-5652.
6. Frisch MJ, Trucks GW, Schlegel HB, Scuseria GE. Gaussian 09, Revision A.02. Gaussian, Inc., Wallingford CT;2009.
7. Johnson BG, Gill PM, Pople JA. The performance of a family of density functional methods,» *The Journal of Chemical Physics.* 1993;98:5612-5626.
8. Hoffmann R, Woodward R. The Conservation of Orbital Symmetry. *J Am Chem Soc.* 1968;1:17-22.
9. Bendjeddou A, Abbaz T, Gouasmia AK, Villemin D. Molecular Structure, HOMO-LUMO, MEP and Fukui Function Analysis of Some TTF-donor Substituted Molecules Using DFT (B3LYP) Calculations. *International Research Journal of Pure & Applied Chemistry.* 2016;12(n° 11).
10. N'dri JS, Koné MR, Kodjo CG, kablan ALC, Affi ST, Ouattara L, Ziao N. Theoretical Study of the Chemical Reactivity of Five Schiff Bases Derived From Dapsone by the DFT Method. *Chemical Science International Journal.* 2018;22(n°14):1-11.

11. Koopmans T. Über die Zuordnung von Wellenfunktionen und Eigenwerten zu den einzelnen Elektronen eines Atoms. *Physica*. 1934;1:104-113.
12. Dheivamalar S, Sugi L, Ambigai K. Density Functional Theory Study of Exohedral Carbon Atoms Effect on Electrophilicity of Nicotine: Comparative Analysis. 2016;17-31.
13. Ayers PW, Parr RG. Variational Principles for Describing Chemical Reactions: The Fukui Function and Chemical Hardness Revisited. *J. Am. Chem. Soc.* 2000;122(n° %19):2010-2018.
14. Fukui K, Yonezawa T, Shingu H. A Molecular Orbital Theory of Reactivity in Aromatic Hydrocarbons,» J. Chem. Phys. 1952;20(n° %14):722-725.
15. Morell C, Grand A, Toro-Labbé A. Theoretical support for using the $\Delta f(r)$ descriptor. *Chem. Phys. Lett.* 2006;425(n° %14-6):342-346.
16. Mekky A, Elhaes H, El-Okr M. Molecular Electrostatic Potential Analysis of Nano-Scale Fullerene (C60) Crystals and Some Specific Derivatives: DFT Approach. *J Nanomater Mol Nanotechnol.* 2006;4: 2015.

© 2022 Tuo et al.; This is an Open Access article distributed under the terms of the Creative Commons Attribution License (<http://creativecommons.org/licenses/by/4.0>), which permits unrestricted use, distribution, and reproduction in any medium, provided the original work is properly cited.

Peer-review history:

The peer review history for this paper can be accessed here:
<https://www.sdiarticle5.com/review-history/81510>